
This copy is for your personal, non-commercial use only.

If you wish to distribute this article to others, you can order high-quality copies for your colleagues, clients, or customers by [clicking here](#).

Permission to republish or repurpose articles or portions of articles can be obtained by following the guidelines [here](#).

The following resources related to this article are available online at www.sciencemag.org (this information is current as of April 8, 2011):

Updated information and services, including high-resolution figures, can be found in the online version of this article at:

<http://www.sciencemag.org/content/332/6026/216.full.html>

Supporting Online Material can be found at:

<http://www.sciencemag.org/content/suppl/2011/04/04/332.6026.216.DC1.html>

This article **cites 16 articles**, 2 of which can be accessed free:

<http://www.sciencemag.org/content/332/6026/216.full.html#ref-list-1>

This article has been **cited by 1** articles hosted by HighWire Press; see:

<http://www.sciencemag.org/content/332/6026/216.full.html#related-urls>

This article appears in the following **subject collections**:

Astronomy

<http://www.sciencemag.org/cgi/collection/astronomy>

- Space Agency–European Southern Observatory (ESA–ESO) Working Group Report no. 4, Paris, 2008].
32. G. Torres, J. Andersen, A. Giménez, *Astron. Astrophys. Rev.* **18**, 67 (2010).
33. P. Marigo *et al.*, *Astron. Astrophys.* **482**, 883 (2008).
34. L. Girardi, M. A. T. Groenewegen, E. Hatziminaoglou, L. da Costa, *Astron. Astrophys.* **436**, 895 (2005).
35. A. Miglio *et al.*, *Astron. Astrophys.* **503**, L21 (2009).
36. Kepler is a NASA discovery class mission, which was launched in March 2009 and whose funding is provided by NASA's Science Mission Directorate. The authors thank the entire Kepler team, without whom these results would not be possible. The asteroseismology program of Kepler is being conducted by the Kepler Asteroseismic Science Consortium.

Supporting Online Material

www.sciencemag.org/cgi/content/full/332/6026/213/DC1
Materials and Methods
Figs. S1 to S3
References

16 December 2010; accepted 22 February 2011
10.1126/science.1201827

HD 181068: A Red Giant in a Triply Eclipsing Compact Hierarchical Triple System

A. Drekas,^{1,2*} L. L. Kiss,^{2,3} T. Borkovits,^{4,5} D. Huber,³ H. Lehmann,⁶ J. Southworth,⁷ T. R. Bedding,³ D. Balam,⁸ M. Hartmann,⁶ M. Hrudkova,⁶ M. J. Ireland,³ J. Kovács,⁹ Gy. Mező,² A. Moór,² E. Niemczura,¹⁰ G. E. Sarty,¹¹ Gy. M. Szabó,² R. Szabó,² J. H. Telting,¹² A. Tkachenko,⁶ K. Uytterhoeven,^{13,14} J. M. Benkő,² S. T. Bryson,¹⁵ V. Maestro,³ A. E. Simon,² D. Stello,³ G. Schaefer,¹⁶ C. Aerts,^{17,18} T. A. ten Brummelaar,¹⁶ P. De Cat,¹⁹ H. A. McAlister,¹⁶ C. Maceroni,²⁰ A. Mérand,²¹ M. Still,¹⁵ J. Sturmann,¹⁶ L. Sturmann,¹⁶ N. Turner,¹⁶ P. G. Tuthill,³ J. Christensen-Dalsgaard,²² R. L. Gilliland,²³ H. Kjeldsen,²² E. V. Quintana,²⁴ P. Tenenbaum,²⁴ J. D. Twicken²⁴

Hierarchical triple systems comprise a close binary and a more distant component. They are important for testing theories of star formation and of stellar evolution in the presence of nearby companions. We obtained 218 days of Kepler photometry of HD 181068 (magnitude of 7.1), supplemented by ground-based spectroscopy and interferometry, which show it to be a hierarchical triple with two types of mutual eclipses. The primary is a red giant that is in a 45-day orbit with a pair of red dwarfs in a close 0.9-day orbit. The red giant shows evidence for tidally induced oscillations that are driven by the orbital motion of the close pair. HD 181068 is an ideal target for studies of dynamical evolution and testing tidal friction theories in hierarchical triple systems.

The Kepler space mission is designed to observe continuously more than 10^5 stars, with the ultimate goal of detecting a sizeable sample of Earth-like planets around main-sequence stars (*I*). We obtained 218 days of Kepler photometry (2–4) of HD 181068 [also Kepler Input Catalog (KIC) 5952403], a star with magnitude $V = 7.1$ and a distance of about 250 pc. It had been previously identified as a single-lined spectroscopic binary (5), but there have been no reports of eclipses.

The data were obtained in long-cadence (LC) mode (one point every 29.4 min) over 218 days using quarters 1, 2, and 3. Our observations reveal a very distinctive light curve. It shows eclipses every ~ 22.7 days and slow variations in the upper envelope (Fig. 1A) that are likely caused by ellipsoidal distortion of the primary component. There are also very regular and much narrower eclipses (Fig. 1B). These minima have alternating depths, corresponding to a close pair (B and C), with an orbital period of ~ 0.9 day. The 22.7-day eclipses all have similar depths, but there are subtle differences between consecutive minima. Radial velocity observations [section 1.2 of (6)] show that the true orbital period of the BC pair around the A component is 45.5 days. The narrow 0.9-day eclipses essentially disappear during both types of the deep minima, implying that the three stars have very similar surface bright-

nesses, so that when the BC pair is in front of A, their mutual eclipses do not change the total amount of light coming from the system (in accordance with the nearly equal depths of the two deep minima). When the BC pair is in front of A, the BC's secondary eclipses appear as tiny brightenings (Fig. 1, D and F), showing that the surface brightness of B is almost equal to that of A, whereas C is a bit fainter, so that its disappearance behind B allows the extra light from A to reach us.

The observed changes in the eclipses of the BC pair and the radial velocity variations of the A component confirm that the A and BC systems are physically associated and not a chance alignment. Their periods are $P_{BC} = 0.90567(2)$ day and $P_{A-BC} = 45.5178(20)$ days (numbers in parentheses refer to the standard error in the last digits). Given the shallow depths of the eclipses, star A must be the most luminous object in the system. In addition to the eclipses, there are brightness fluctuations during the long-period minima that imply that component A is also an intrinsic variable star with a mean cycle length close to half the shorter orbital period, possibly indicating tidally induced oscillations.

In addition, there were several flarelike events in the light curve that usually lasted about 6 to 8 hours. We checked the Kepler Data Release Notes (7) for documented instrumental effects in the vicinity of the “flares” but found none. More-

over, almost all flares appear right after the shallower minimum of the BC pair, suggesting that this activity might be related to the close pair.

We looked for optically resolved companion(s) with a 1-m telescope [section 1.1 of (6)] but found none. We also obtained 38 high-resolution optical spectra to measure the orbital reflex motion of the A component (6) (fig. S1). The orbital parameters for the wider system (Table 1) reveal that star A revolves on a circular orbit, which has an orbital period twice the separation of the two consecutive flat-bottomed minima in the light curve (6). Long-baseline interferometry using the PAVO (Precision Astronomical Visible Observations) beam combiner (8) at the CHARA [Center for High Angular Resolution Astronomy (9)] Array show that the angular diameter of HD

¹Department of Astronomy, Eötvös University, Budapest, Hungary. ²Konkoly Observatory, Hungarian Academy of Sciences, H-1525 Budapest, Post Office Box 67, Hungary. ³Sydney Institute for Astronomy, School of Physics, University of Sydney, Sydney, NSW 2006, Australia. ⁴Baja Astronomical Observatory, H-6500 Baja, Szegedi út, Kt. 766, Hungary. ⁵Eötvös József College, H-6500 Baja, Szegedi út 2, Hungary. ⁶Thüringer Landessternwarte (TLS) Tautenburg, Karl-Schwarzschild-Observatorium, 07778 Tautenburg, Germany. ⁷Astrophysics Group, Keele University, Newcastle-Under-Lyme ST5 5BG, UK. ⁸Dominion Astrophysical Observatory (DAO), Herzberg Institute of Astrophysics, 5071 West Saanich Road, Victoria, BC V9E 2E7, Canada. ⁹Gothard Observatory, Eötvös University, H-9704 Szombathely, Szent Imre Herceg u. 112., Hungary. ¹⁰Astronomical Institute, Wrocław University, Kopernika 11, 51-622 Wrocław, Poland. ¹¹Department of Physics and Engineering Physics, University of Saskatchewan, 9 Campus Drive, Saskatoon, Saskatchewan S7N 5A5, Canada. ¹²Nordic Optical Telescope, Apartado 474, 38700 Santa Cruz de La Palma, Spain. ¹³Laboratoire Astrophysique, Instrumentation, et Modélisation, Commissariat à l'Energie Atomique (CEA)/Direction des Sciences de la Matière–CNRS–Université Paris Diderot; CEA, l'institut de recherche sur les lois fondamentales de l'Univers, Service d'Astrophysique, Saclay, 91191, Gif-sur-Yvette, France. ¹⁴Kiepenheuer-Institut für Sonnenphysik, Schöneckstrasse 6, 79104 Freiburg, Germany. ¹⁵National Aeronautics and Space Administration (NASA) Ames Research Center, Moffett Field, CA 94035, USA. ¹⁶Center for High Angular Resolution Astronomy, Georgia State University, Post Office Box 3969, Atlanta, GA 30302–3969, USA. ¹⁷Instituut voor Sterrenkunde, Katholieke Universiteit Leuven, Celestijnenlaan 200 D, 3001 Leuven, Belgium. ¹⁸Institute for Mathematics, Astrophysics, and Particle Physics (IMAPP), Department of Astrophysics, Radboud University Nijmegen, Post Office Box 9010, NL-6500 GL Nijmegen, Netherlands. ¹⁹Royal Observatory of Belgium, Ringlaan 3, 1180 Brussels, Belgium. ²⁰Istituto Nazionale di Astrofisica (INAF), Osservatorio astronomico di Roma, via Frascati 33, I-00040 Monteporzio C., Italy. ²¹European Southern Observatory, Alonso de Córdova 3107, Casilla 19001, Santiago 19, Chile. ²²Department of Physics and Astronomy, Building 1520, Aarhus University, 8000 Aarhus C, Denmark. ²³Space Telescope Science Institute, 3700 San Martin Drive, Baltimore, MD 21218, USA. ²⁴SETI Institute, Moffett Field, CA 94035, USA.

*To whom correspondence should be addressed. E-mail: derekas@konkoly.hu

Fig. 1. Kepler-band light curves of HD 181068 from observations in LC mode: **(A)** the full 218 days and **(B)** a 28-day segment showing two consecutive deep minima. Time is expressed in barycentric Julian date. **(C to F)** Close-ups of two secondary minima and two primary minima of the 45.5-day eclipses. The dashed and dotted lines mark the primary and the secondary minima of the 0.9-day eclipses, respectively. The discontinuities in **(A)** correspond to the telescope rolls at the end of each quarter.

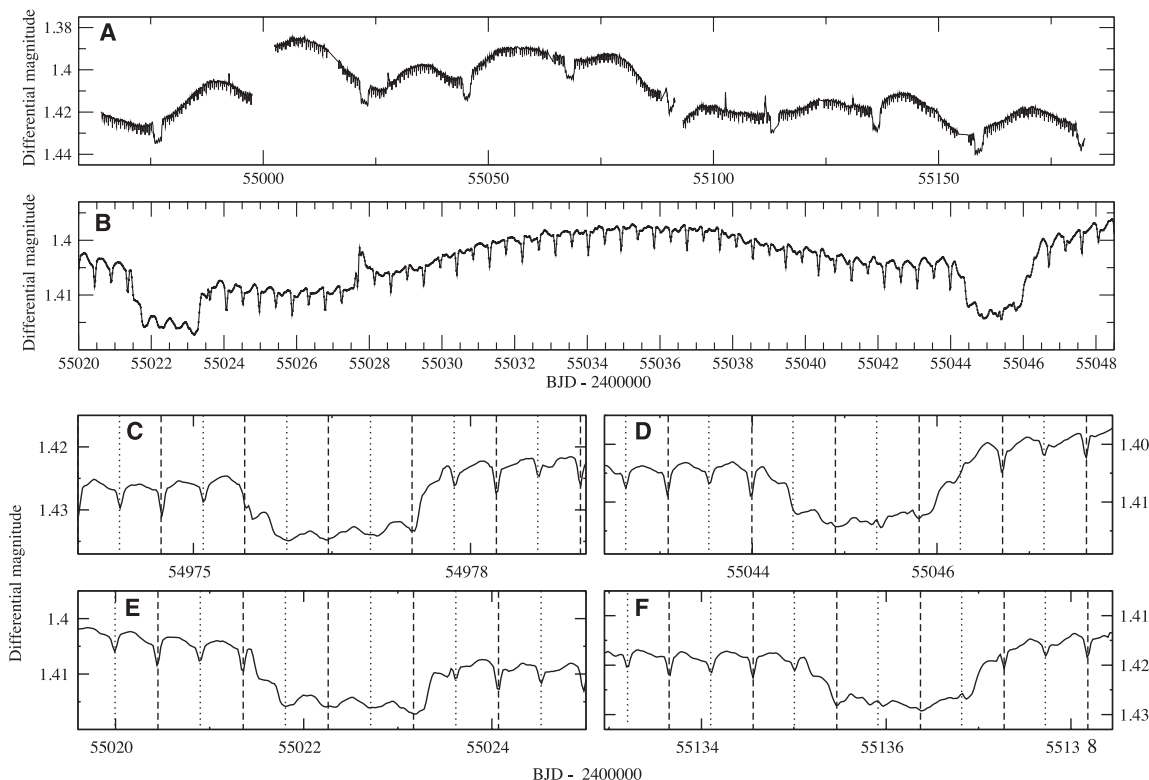


Table 1. Orbital elements for the wider system derived from the A component's radial velocity curve (fig. S1). K_2 , the velocity amplitude of component A; v_γ , the center-of-mass velocity of the system; e_2 , the eccentricity of the wide pair; $f(m)$, the mass function.

Element	Value
P_{A-BC}	45.5178 days (fixed)
$T_{\text{Min } 1}$	$2,455,454.573 \pm 0.095$ (fixed)
K_2	$37.195 \pm 0.053 \text{ km s}^{-1}$
v_γ	$6.993 \pm 0.011 \text{ km s}^{-1}$
e_2	0.0 (fixed)
$f(m)$	$0.24 \pm 0.02 M_\odot$

181068 A, corrected for limb darkening (10), is $\theta_{\text{LD}} = 0.461 \pm 0.011$ milli-arc sec (mas) (Fig. 2) [see (6) for details].

Combining the measured angular diameter with the Hipparcos parallax of 4.0 ± 0.4 mas (11), we find the linear radius of the primary component to be $R = 12.4 \pm 1.3 R_\odot$ (where R_\odot is the radius of the Sun). With use of the spectroscopically determined $T_{\text{eff}} = 5100 \pm 200$ K, this implies a luminosity of $L = 93 \pm 19 L_\odot$ (where L_\odot is the luminosity of the Sun). This value matches that found from the Hipparcos parallax and the apparent magnitude. We also estimated the absolute magnitude of HD 181068 A on the basis of the Wilson-Bappu effect (12), which correlates the width of the chromospheric Ca II K emission line at 3934 Å with the V -band absolute magnitude. With the latest calibration (13), the measured width of the emission core, $W_0 = 72.8 \text{ km s}^{-1}$ (6), implies an absolute brightness of $M_V = -0.3$ mag-

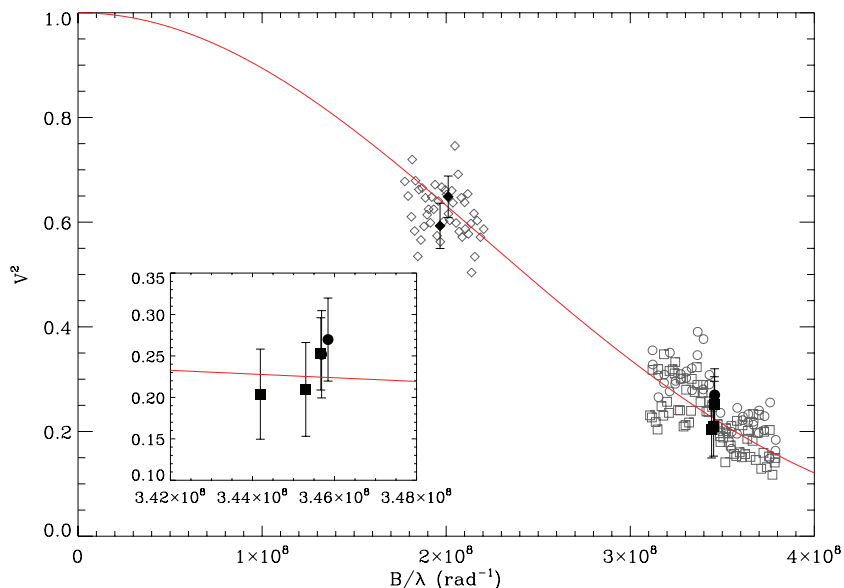


Fig. 2. Squared visibility versus spatial frequency (projected baseline length over wavelength) from PAVO on CHARA. Gray points show all collected measurements; black symbols show the average of each scan over all wavelength channels; the error bars show the standard error of the mean. Each symbol type corresponds to a different night of observations. The solid line is the best-fitting model. **(Inset)** A close-up of the observations at the longer baselines.

nitude, which matches the parallax and the interferometric results.

We estimated the mass of HD 181068 A by comparing the effective temperature and the luminosity with evolutionary tracks from the BASTI database (14). We obtained $M_A \sim 3.0 \pm 0.4 M_\odot$ (where M_\odot is the mass of the Sun), corresponding to a red giant, possibly in the He-core burning

phase of its evolution (15). The full spectral energy distribution constructed by using all published broad-band optical magnitudes and infrared flux values (6) does not show any excess in comparison to a 5200-K photospheric model, indicating that no detectable circumstellar dust, possibly from mass-loss processes on the red giant branch, is present.

We have constrained the parameters of the BC pair by modeling the short-period eclipses in the Kepler band using the jktebop code (16, 17). The ratio of the radii of the B and C components is poorly constrained at present, partly because of the low sampling rate of the Kepler LC data. The A component contributes 99.29% of the system light in the Kepler passband, and the BC pair contribute 0.44% and 0.27%, respectively. Taking the *V*-band absolute magnitude of HD 181068 A to be $M_V(A) = -0.3$ and assuming that our results for the Kepler passband are representative of the *V* band, we find $M_V(B) = 5.6$ and $M_V(C) = 6.1$. Such absolute magnitudes indicate spectral types of G8 V and K1 V for stars B and C, respectively (18). Because we do not have independent measurements of T_{eff} for the BC pair, we can only estimate their masses based on their spectral types. This indicates that their masses are about $0.7 \pm 0.1 M_{\odot}$ each (6).

One puzzling feature of the system is the short-period fluctuations that have the largest amplitudes when the BC pair is behind star A, while remaining apparent with a slowly changing amplitude in all the other phases of the wide orbit. We have investigated this variability of HD 181068 A with a detailed frequency analysis and a comparison to other red giant stars that have similar properties (6). The frequency content of the light curve suggests an intimate link to tidal effects in the triple system, with the first four dominant peaks in the power spectrum identifiable as simple linear combinations of the two orbital frequencies. On the other hand, solarlike oscillations (meaning those excited by near-surface convection, as in the Sun but also observed in red giants) that are expected to produce an equidistant series of peaks in the power spectrum are not visible, even though all stars with similar parameters in the Kepler database do show clear evidence of these oscillations. In other words, the convectively driven solarlike oscillations that we would expect to see in a giant of this type seem to have been suppressed (6).

In a recent compilation of 724 triple stars (19), there is only one system with an outer orbital period shorter than that of HD 181068 (λ Tau, for which $P_{\text{out}} = 33.03$ days). Carter *et al.* (20) reported the discovery of KOI-126 with a similarly short outer period ($P_{\text{out}} = 33.92$ days). Extremely compact hierarchical triple systems form a very small minority of hierarchical triplets, with only 7 of the catalogized 724 systems having outer periods shorter than 150 days. Furthermore, HD 181068 and KOI-126 have the highest outer mass ratios [~ 2.1 and 3, defined as $m_A/(m_B + m_C)$] among the known systems. In 97% of the known hierarchical triplets before the Kepler era, the mass of the close binary exceeded that of the wider companion, and even the largest outer mass ratio remained under 1.5. It is not yet clear whether this rarity of such systems is caused by an observational selection effect or has an underlying stellar evolutionary or dynamical explanation.

Its properties make HD 181068 an ideal target for dynamical evolutionary studies and for testing tidal friction theories. Because of its compactness and its massive primary, we can expect short-term orbital element variations on two different time scales of 46 days (i.e., with period of P_{A-BC}) and about 6 years (P_{A-BC}^2/P_{BC}), the time scale of the classical apsidal motion and nodal regression (21), which for the triply eclipsing nature could be observed relatively easily.

References and Notes

- W. J. Borucki *et al.*, *Science* **327**, 977 (2010).
- D. G. Koch *et al.*, *Astrophys. J.* **713**, L79 (2010).
- J. M. Jenkins *et al.*, *Astrophys. J.* **713**, L87 (2010).
- J. M. Jenkins *et al.*, *Astrophys. J.* **713**, L120 (2010).
- P. Guillout *et al.*, *Astron. Astrophys.* **504**, 829 (2009).
- Materials and methods are available as supporting material on Science Online.
- Available at <http://archive.stsci.edu/kepler/>.
- M. J. Ireland *et al.*, in *Optical and Infrared Interferometry*, M. Scholler, W. C. Danchi, F. Delplancke, Eds., vol. 7013 of *Proceedings of the SPIE* (Society of Photo-Optical Instrumentation Engineers, Bellingham, WA, 2008), pp. 701324–701324-10.
- T. A. ten Brummelaar *et al.*, *Astrophys. J.* **628**, 453 (2005).

- R. Hanbury Brown *et al.*, *Mon. Not. R. Astron. Soc.* **167**, 475 (1974).
- F. van Leeuwen, *Hipparcos, the New Reduction of the Raw Data* (Astrophysics and Space Science Library, Springer, Berlin, 2007), vol. 350.
- O. C. Wilson, M. K. V. Bappu, *Astrophys. J.* **125**, 661 (1957).
- G. Pace, L. Pasquini, S. Ortolani, *Astron. Astrophys.* **401**, 997 (2003).
- A. Pietrinferni, S. Cassisi, M. Salaris, F. Castelli, *Astrophys. J.* **612**, 168 (2004).
- L. Girardi, *Mon. Not. R. Astron. Soc.* **308**, 818 (1999).
- J. Southworth, S. Zucker, P. F. L. Maxted, B. Smalley, *Mon. Not. R. Astron. Soc.* **355**, 986 (2004).
- J. Southworth, B. Smalley, P. F. L. Maxted, A. Claret, P. B. Etzel, *Mon. Not. R. Astron. Soc.* **363**, 529 (2005).
- A. N. Cox, *Allen's Astrophysical Quantities* (Springer, New York, 2000).
- A. A. Tokovinin, *Mon. Not. R. Astron. Soc.* **389**, 925 (2008).
- J. A. Carter *et al.*, *Science* **331**, 562 (2011); [10.1126/science.1201274](https://doi.org/10.1126/science.1201274).
- E. W. Brown, *Mon. Not. R. Astron. Soc.* **97**, 62 (1936).
- A.D. is a Magyary Zoltán Postdoctoral Research Fellow. Funding for this Discovery mission is provided by NASA's Science Mission Directorate. The authors gratefully acknowledge the entire Kepler team, whose outstanding efforts have made these results possible. This project has been supported by Hungarian Scientific Research Fund (OTKA) grants K76816, K83790, and MB08C 81013; the "Lendület" Program of the Hungarian Academy of Sciences; and the Magyary Zoltán Higher Educational Public Foundation. The DAO observations were supported by an American Astronomical Society Small Research Grant. The CHARA Array is owned by Georgia State University. Additional funding for the CHARA Array is provided by NSF under grant AST09-08253, the W. M. Keck Foundation, and the NASA Exoplanet Science Center. TLS observations were done as a part of the Deutsche Forschungsgemeinschaft grant HA 3279/5-1. For her research, C.A. received funding from the European Research Council (ERC) under the European Community's Seventh Framework Programme (FP7/2007-2013)/ERC grant agreement no. 227224 (Prosperity).

Supporting Online Material

www.sciencemag.org/cgi/content/full/332/6026/216/DC1
Materials and Methods
Figs. S1 to S3
Tables S1 to S3
References
SOM Data

15 December 2010; accepted 3 March 2011
[10.1126/science.1201762](https://doi.org/10.1126/science.1201762)

Surface-Plasmon Holography with White-Light Illumination

Miyu Ozaki,^{1,2} Jun-ichi Kato,¹ Satoshi Kawata^{1,3*}

The recently emerging three-dimensional (3D) displays in the electronic shops imitate depth illusion by overlapping two parallax 2D images through either polarized glasses that viewers are required to wear or lenticular lenses fixed directly on the display. Holography, on the other hand, provides real 3D imaging, although usually limiting colors to monochrome. The so-called rainbow holograms—mounted, for example, on credit cards—are also produced from parallax images that change color with viewing angle. We report on a holographic technique based on surface plasmons that can reconstruct true 3D color images, where the colors are reconstructed by satisfying resonance conditions of surface plasmon polaritons for individual wavelengths. Such real 3D color images can be viewed from any angle, just like the original object.

Noble metal films, such as silver and gold foil, contain free electrons that collectively oscillate and propagate as the surface

wave in optical frequency region. The quantum of this surface wave is called surface plasmon polariton (SPP) (1). The electromagnetic field gen-

erated by SPP can be enhanced and strongly confined spatially in the near field (with the distance less than the wavelength) from the metal surface as a nonirradiative evanescent field (2, 3). The ability to confine and enhance the optical field to the vicinity of the metal surface or nanometal particle has been applied to immuno-sensor (4), fluorescence sensor (5), solar cell (6), plasmonic laser (7, 8), nanomicroscopy (9, 10), super-lens (11, 12) and photodynamic cancer cell treatment (13).

We report an application of SPP to three-dimensional (3D) color holography with white-

¹RIKEN, Wako, Saitama 351-0198, Japan. ²Department of Robotics and Mechatronics, Tokyo Denki University, Chiyoda-ku, Tokyo 101-8457, Japan. ³Department of Applied Physics and Photonics Advanced Research Center, Osaka University, Suita, Osaka, 565-0871, Japan.

*To whom correspondence should be addressed. E-mail: kawata@skawata.com